Scattering of electromagnetic waves by arbitrarily shaped dielectric bodies

P. Barber and C. Yeh

The differential scattering characteristics of closed three-dimensional dielectric objects are theoretically investigated. The scattering problem is solved in a spherical basis by the Extended Boundary Condition Method (EBCM) which results in a system of linear equations for the expansion coefficients of the scattered field in terms of the incident field coefficients. The equations are solved numerically for dielectric spheres, spheroids, and finite cylinders to study the dependence of the differential scattering on the size, shape, and index of refraction of the scattering object. The method developed here appears to be most applicable to objects whose physical size is on the order of the wavelength of the incident radiation.

I. Introduction

The calculation of the scattering of electromagnetic waves by dielectric objects is a problem that has received increased attention in recent years. Knowledge of the scattered field is required in many areas, such as in investigations of the scattering of microwaves by raindrops and the scattering of light by small chemical and biological particles. The solution of the scattering problem for spherical objects is well known (the Mie theory) and has been used to great advantage in the study of many physical systems. However, many investigations are concerned with the scattering by nonspherical bodies, and the need for a method to determine rapidly the theoretical scattering by nonspherical objects is clearly indicated. Furthermore, a primary need is for methods that are applicable to objects whose physical size is on the order of the wavelength of the incident radiation (the so-called resonance region). This paper will be concerned with the solution of the scattering problem for nonspherical dielectric bodies. The method is most applicable to objects lying in the electromagnetics resonance region. The theoretical equations will be solved numerically for common solid geometric shapes to study the dependence of the scattering on the size, shape, and index of refraction of the scattering object.

When this work was done, both authors were with the University of California, Electrical Sciences & Engineering Department, School of Engineering & Applied Science, Los Angeles, California 90024. P. Barber is now with the University of Utah, Salt Lake City, Utah 84112.

Received 23 September 1974.

Many techniques have been developed for analyzing scattering and diffraction problems involving dielectric obstacles. Each of the available methods generally has a range of applicability that is determined by the size of the scattering object relative to the wavelength of the incident radation. The scattering by objects that are very small compared to the wavelength can be analyzed by the Rayleigh approximation,[1] and geometrical optics methods can be employed for objects that are electrically large.[2,3] Objects whose size is on the order of the wavelength of the incident radiation lie in the range commonly called the resonance region, and the complete wave nature of the incident radiation must be considered in the solution of the scattering problem.

The classical method of solution in the resonance region utilizes the separation of variables technique. This is only effective for bodies whose bounding surface coincides with one of the coordinate systems for which the vector Helmholtz equation is separable, and therefore its application has been restricted to infinite circular[4] and elliptic cylinders[5] in two dimensions and to the sphere[6] (the Mie theory) in three dimensions. Other methods that have been used to solve dielectric scattering problems in the resonance region include point matching methods and perturbation techniques. The point matching method[7,8] assumes a spherical expansion (or circular cylindrical expansion in two dimensions) of the scattered field is valid on the surface of a nonspherical body. The perturbation technique[9] considers a nonspherical body as a distortion (perturbation) of a perfect sphere. It is most effective for bodies that are only slightly nonspherical. Various integral equation[10,11] formulations have also been quite successful for solving dielectric scattering problems. Based on exact

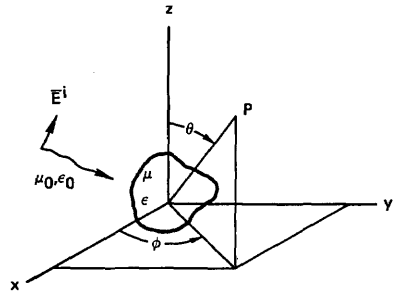

Fig. 1. Scattering geometry.

theory, these methods are quite general and are very amenable to solution by digital computer.

A new matrix formulation of scattering, which could be classified as an integral equation method, has recently been developed by Waterman.[12–15] Originally published for conducting bodies,[12,13] this method, called the Extended Boundary Condition Method, is exact and provides a general formulation for scattering from obstacles of arbitrary size and shape with size ratios from the Rayleigh region to the geometric optics limit. Waterman later extended the theory to dielectric obstacles[14] using the vector Huygen's principle.[16]

The present investigation begins with a theoretical development of the Extended Boundary Condition Method as it applies to scattering by dielectric objects. It will be shown that an alternate, but conceptually similar derivation, results using Schelkunoff's equivalence theorem,[17] rather than the Huygen's principle.

The over-all goal is to determine the scattered field when an arbitrary dielectric body is illuminated by a plane electromagnetic wave as shown in Fig. 1. Specifically, we wish to compute the differential scattering, which is the complete scattering pattern in all directions due to an incident wave in one particular direction. The dielectric body, assumed homogeneous and isotropic, is characterized by the constitutive parameters μ, ϵ, where μ is the permeability, and ϵ is the permittivity of the dielectric material (ϵ may be complex to account for the lossy case). The surrounding medium is considered to be free space with parameters μ_0, ϵ_0. The scattered field must be determined for all locations P on a sphere surrounding the scattering object.

The scattering problem is illustrated schematically in Fig. 2. The total field everywhere is given by the sum of the incident field and the scattered field, where the incident field $\bar{E}^i$, $\bar{H}^i$ is the field present in the absence of the scatterer, and the scattered field $\bar{E}^s$, $\bar{H}^s$ is given by the difference between the field with the object present ($\bar{E}$, $\bar{H}$) and the incident field, that is,

$$\bar{E}^s = \bar{E} - \bar{E}^i, \bar{H}^s = \bar{H} - \bar{H}^i. \quad (1)$$

This scattered field can be thought of as the field produced by polarization currents within the scattering object.

The goal of the theoretical development is to find a solution for the scattered field in terms of the incident field and the physical characteristics of the scattering object. This is accomplished by an application of the equivalence theorem which casts the scattered field as due to a set of surface currents located coincident with the surface of the scattering object. The remainder of the analysis then consists of finding an expression for these surface currents. The approach followed ultimately finds the internal fields in terms of the incident field, then the surface currents in terms of the internal fields, and finally the scattered field as a function of these surface currents. The entire analysis can conveniently be broken down into the following steps:

(1) The equivalence theorem is applied, which, as far as the external fields are concerned, effectively replaces the scattering object by a set of surface currents over S. These surface currents, which are derived from the tangential components of the external field, are found to be the source of the scattered field outside S, and because the equivalence theorem results in a null field inside S, they radiate a scattered field within S that cancels the incident field.

(2) The problem resulting from the application of the equivalence theorem is analyzed. This problem is called the external problem, because the fields external to S are the same as in the original problem. One expression for the unknown surface currents in terms of the incident field is derived from the fact that these surface currents radiate a scattered field that cancels the incident field throughout the interior volume. These equations are put in a form suitable for numerical solution by expansion of the various field quantities in vector spherical wave functions.

(3) Considering the complete problem again, the fields internal to the dielectric region are now expanded in regular vector spherical wave functions with coefficients to be determined.

(4) The boundary conditions at the surface are applied, and the continuity of the tangential fields leads to the linear system of integral equations for the coefficients of the unknown internal fields in terms of the expansion coefficients of the incident field.

(5) The scattered far field is then determined by evaluating the internal field at the surface and then

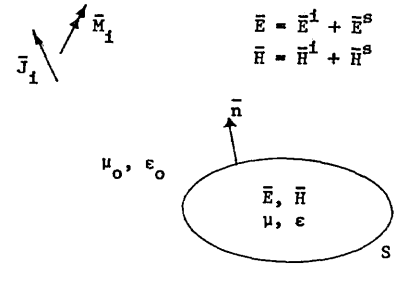

Fig. 2. The scattering problem. $\bar{J}_i$ and $\bar{M}_i$ are the sources of the incident field.

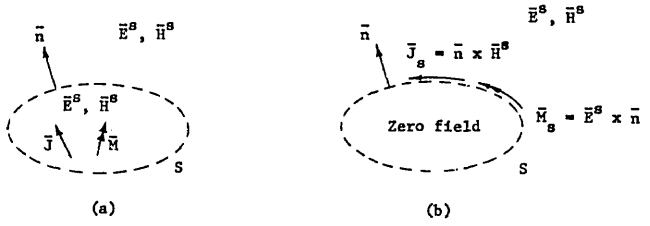

Fig. 3. Application of the equivalence theorem to the scattered field sources.

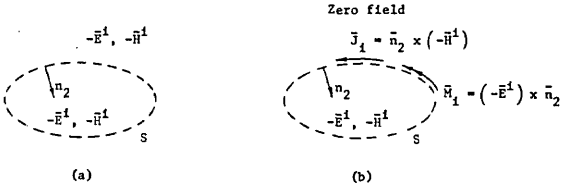

Fig. 4. Application of the equivalence theorem to the negative of the incident field sources.

solving for the scattered field in terms of the surface fields. The differential scattering cross section is proportional to the square of the far field amplitude.

II. Application of the Equivalence Principle

Let a closed surface S separate an isotropic homogenous medium into two regions as shown in Fig. 3(a). All the sources are contained within S so that the region outside S is source-free. Schelkunoff's equivalence theorem states that the field in a source-free region bounded by a surface S could be produced by a distribution of electric and magnetic currents on this surface, and, in this sense, the actual source distribution can be replaced by an equivalent distribution. Furthermore, if the field produced by the original source is $\bar{E}^s$, $\bar{H}^s$, the equivalent sources on S consist of an electric current sheet of density $\bar{n} \times \bar{H}^s$ and a magnetic current sheet of density $\bar{E}^s \times \bar{n}$, where the normal $\bar{n}$ points from the region containing the sources to the source-free region. The application of Schelkunoff's equivalence theorem is shown in Fig. 3(b). Note that the boundary conditions at S indicate that the surface currents produce a null field within S.

We relate the situation shown in Fig. 3 to the scattered field portion of our scattering problem by identifying $\bar{J}$ and $\bar{M}$ in Fig. 3(a) as polarization currents[17] within S (which have been induced by an incident field), which radiate in free space to produce the scattered field $\bar{E}^s$, $\bar{H}^s$. In Fig. 3(b), these polarization currents have been replaced by equivalent surface currents that radiate the scattered field external to S and a null field inside S.

Now we go through some additional transformations to construct the complete scattering problem as a sum of fields due to different sources.

Consider the situation depicted in Fig. 4(a). Here we have a set of sources $-\bar{J}_i$, $-\bar{M}_i$ radiating in free space and producing a field $-\bar{E}^i$, $-\bar{H}^i$. The equivalene theorem can be applied as shown in Fig. 4(b) so that the sources outside S can be replaced by equivalent surface currents on S, which radiate the fields $-\bar{E}^i$, $-\bar{H}^i$ within S and a null field outside S. Relative to the total scattering problem, we identify these fields as the negative of the incident field.

We now apply superposition and add together the sources and fields from Figs. 3(b) and 4(b), obtaining the situation shown in Fig. 5(a). Here we end up with a set of surface currents that radiate the scattered field external to S and the negative of the incident field internal to S. If we now add to Fig. 5(a) a set of sources $\bar{J}_i$, $\bar{M}_i$ producing an incident field $\bar{E}^i$, $\bar{H}^i$, we obtain the configuration shown in Fig. 5(b). $\bar{E}_+$ and $\bar{H}_+$ are the values of the external $\bar{E}$, $\bar{H}$ fields at the surface. It can be seen that external to the surface S, the sources and fields are exactly the same as those existing in the original scattering problem, and we have replaced the scattering object by a set of surface currents over a surface S. Furthermore, these surface currents radiate in unbounded free space to produce the scattered field outside S and the negative of the incident field inside S.

III. External Problem

Referring to Fig. 5(b), the entire region is unbounded, and, therefore, the scattered fields everywhere due to $\bar{J}_+$ and $\bar{M}_+$ can be determined from the vector potentials $\bar{A}$ and $\bar{F}$.[4]

$$\bar{E}^s = -\nabla \times \bar{F} - \frac{1}{j\omega\epsilon_0}(\nabla \times \nabla \times \bar{A}), \tag{2a}$$

$$\bar{H}^s = \nabla \times \bar{A} - \frac{1}{j\omega\mu_0}(\nabla \times \nabla \times \bar{F}), \tag{2b}$$

where

$$\bar{A} = \frac{1}{4\pi}\int_s \frac{\bar{J}_+ \exp(jk|\bar{r} - \bar{r}'|)}{|\bar{r} - \bar{r}'|}\, dS, \quad \bar{J}_+ = \bar{n} \times \bar{H}_+ \tag{3a}$$

and

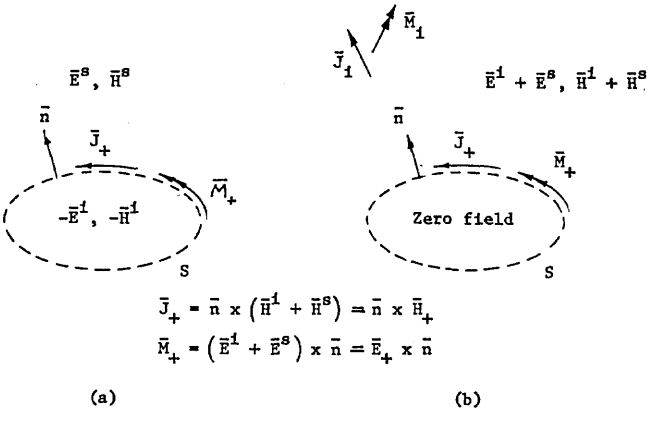

Fig. 5. Summing of sources and fields to obtain the external problem: (a) the sum of Figs. 3(b) and 4(b); (b) adding in the incident sources and fields.

$$\bar{F} = \frac{1}{4\pi}\int_s \frac{\bar{M}_+ \exp(jk|\bar{r} - \bar{r}'|)}{|\bar{r} - \bar{r}'|} dS, \bar{M}_+ = \bar{E}_+ \times \bar{n}; \quad (3b)$$

$\bar{r}'$ and $\bar{r}$ are position vectors from an interior origin to source and field points, respectively, and an $e^{-j\omega t}$ time variation has been assumed. The expression for the scattered electric field can be obtained by substituting Eqs. (3a) and (3b) into Eq. (2a).

$$\bar{E}^s(\bar{r}) = \nabla \times \int_s (\bar{n} \times \bar{E}_+) g(kR) dS - \nabla \times \nabla \times \int_s \frac{1}{j\omega\epsilon_0} (\bar{n} \times \bar{H}_+) g(kR) dS, \quad (4)$$

where $g(kR)$ is the free space Green's function $[\exp(jkR)]/(4\pi R)$

$$R = |r - r'| \text{ and } k = 2\pi/\lambda.$$

The expression for the total field is given by

$$\left.\begin{matrix}\bar{E}(\bar{r}) \\ 0\end{matrix}\right\} = \bar{E}^i(\bar{r}) + \nabla \times \int_s (\bar{n} \times \bar{E}_+) g(kR) dS - \nabla \times \nabla \times \int_s \frac{1}{j\omega\epsilon_0} (\bar{n} \times \bar{H}_+) g(kR) dS; \bar{r} \begin{cases}\text{outside } S \\ \text{inside } S.\end{cases} \quad (5)$$

It can be seen that for $\bar{R}$ inside S, Eq. (5) partially determines the surface currents because of the requirement that the scattered field must cancel the incident field throughout the interior volume as previously indicated, i.e., for $\bar{r}$ inside S,

$$\nabla \times \int_s (\bar{n} \times \bar{E}_+) g(kR) dS - \nabla \times \nabla \times \int_s \frac{1}{j\omega\epsilon_0} (\bar{n} \times \bar{H}_+) g(kR) dS = -\bar{E}^i(\bar{r}). \quad (6)$$

This equation can be expanded by making use of the spherical vector harmonics $\bar{M}$ and $\bar{N}$ which have been defined by Stratton.[6] These functions, solutions of the vector wave equation, are given by

$$\bar{M}_{emn}(\bar{r}) = \nabla \times \bar{r} \begin{matrix}\cos m\phi \\ \sin m\phi\end{matrix} P_n^m(\cos\theta) z_n(kr) \quad (7a)$$

$$\bar{N}_{emn}(\bar{r}) = \frac{1}{k} \nabla \times \bar{M}_{emn}(\bar{r}), \quad (7b)$$

where

e = even or odd;
$P_n^m(\cos\theta)$ = associated Legendre function;
$z_n(kr)$ = an appropriate spherical Bessel function.

For solutions of the wave equation that must be finite at $r = 0$, $z_n(kr) = j_n(kr)$, and the resulting vector spherical functions $\bar{M}$ and $\bar{N}$ are known as solutions of the first kind. The other vector spherical functions we will be using are obtained by using the spherical Hankel functions, i.e., $z_n(kr) = h_n^{(1)}(kr) = j_n(kr) + jn_n(kr)$. This solution, representing outgoing waves, is called the solution of the third kind.

Using these spherical vector harmonics, the incident field is given by

$$\bar{E}^i(\bar{r}) = \sum_{\nu=1}^{\infty} D_\nu [a_\nu \bar{M}_\nu^1(k\bar{r}) + b_\nu \bar{N}_\nu^1(k\bar{r})], \quad (8)$$

where ν is a combined index incorporating σ, m, and n. D_ν is a normalization constant, and the expansion coefficients a_ν and b_ν are known for a specified incident field.

$$D_\nu = \epsilon_m \frac{(2n+1)(n-m)!}{4n(n+1)(n+m)!}, \quad \epsilon_m = \begin{matrix}1 \\ 2\end{matrix}, \begin{matrix}m = 0 \\ m > 0.\end{matrix}$$

The terms in the integrals of Eq. (6) are expanded as follows:

$$(\bar{n} \times \bar{E}_+) g(kR) = (\bar{n} \times \bar{E}_+) \cdot \bar{\bar{G}}, \quad (9a)$$

$$(\bar{n} \times \bar{H}_+) g(kR) = (\bar{n} \times \bar{H}_+) \cdot \bar{\bar{G}}, \quad (9b)$$

where $\bar{\bar{G}}(kR)$ is the free space Green's dyadic given by Morse and Feshbach.[18]

$$\bar{\bar{G}}(kr) = \frac{jk}{\pi} \sum_{\nu=1}^{\infty} D_\nu [\bar{M}_\nu^3(k\bar{r}_>) \bar{M}_\nu^1(k\bar{r}_<) + \bar{N}_\nu^3(k\bar{r}_>) \bar{N}_\nu^1(k\bar{r}_<)], \quad (10)$$

$\bar{r}_>$, $\bar{r}_<$ are, respectively, the greater and lesser of $\bar{r}$, $\bar{r}'$. The irrotational terms normally present in Eq. (10) are not specified as they will wash out due to the curl operation in Eq. (6).

Equation (6) is required to hold throughout the entire interior volume, i.e., for all r inside S. Now we wish to substitute the expansions of Eq. (8) through Eq. (10) into Eq. (6). Before this is done, the region of convergence of the expansions of Eqs. (8) and (10) should be investigated. The series expansion for the incident field given in Eq. (8) obviously has no singularities within the interior volume, but the same cannot be said for the Green's function expansion in Eq. (10); $g(kR) = [\exp(jkR)]/(4\pi R)$ has a singularity at $R = 0$, i.e., for $\bar{r} = \bar{r}'$. Therefore, an expansion about an origin in the enclosed volume is valid only within an inscribed sphere (and outside a circumscribed sphere), as shown in Fig. 6.

For the moment, restrict the field point $\bar{r}$ to lie within the inscribed sphere. Substituting Eq. (8) through Eq. (10) into Eq. (6) gives the following set of equations:

$$\frac{jk^2}{\pi} \int_S \left[\bar{N}_\nu^3(k\bar{r}') \cdot (\bar{n} \times \bar{E}_+) + j\left(\frac{\mu_0}{\epsilon_0}\right)^{1/2} \bar{M}_\nu^3(k\bar{r}') \cdot (\bar{n} \times \bar{H}_+)\right] dS = -a_\nu; \quad (11a)$$

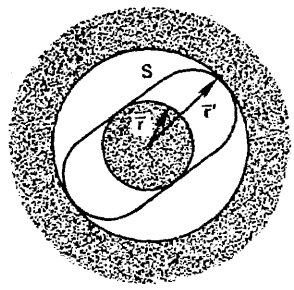

Fig. 6. Region of convergence of the Green's function expansion (shaded).

$$\frac{ik^2}{\pi}\int_s \Big[\bar{M}_\nu^3(k\bar{r}')\cdot(\bar{n}\times\bar{E}_+) + j\left(\frac{\mu_0}{\epsilon_0}\right)^{1/2}\bar{N}_\nu^3(k\bar{r}')\cdot(\bar{n}\times\bar{H}_+)\Big]\,ds = -b_\nu; \quad (11b)$$

where $\nu = 1, 2, 3, \ldots$.

Note that the substitution into Eq. (6) has resulted in two sets of equations. The reason for this is that the coefficient of each regular wave function ($\bar{M}$ or $\bar{N}$) must vanish separately due to the orthogonality of the functions over a spherical surface about the origin.

The solution of Eqs. (11) guarantees that the total field will be zero within the inscribed sphere, but we need to guarantee a null field throughout the entire interior volume. As shown by Waterman,[12] this can be accomplished by using the concept of analytic continuation.

From the theory of complex variables, if an analytic function can be expanded in a region with a finite radius of convergence, that function can also be expanded about any origin within the original region of convergence out to the nearest singularity of the function. This process can be repeated, resulting in the analytic continuation of the function from its original region of definition to other parts of the enclosed volume.[19] The result is that the solution of Eqs. (11), which guarantees zero total field within the inscribed sphere, is sufficient to guarantee that the total field is zero within the entire enclosed volume.

It should be noted that Eqs. (11) can be solved for $\bar{n}\times\bar{E}_+$ and $\bar{n}\times\bar{H}_+$ (the surface currents). These surface currents can then be substituted into Eq. (4) to determine the scattered field, but this scattered field is the result for the external problem alone, which by now is recognized as the problem of scattering by a perfect conductor. The external problem represents only half of the problem for dielectric scattering, and the other half, the internal problem, must now be considered.

IV. Internal Problem

Assume that the field inside the dielectric can be approximated by

$$\bar{E}(k'\bar{r}) = \sum_{\mu=1}^{N}[c_\mu\bar{M}_\mu^1(k'\bar{r}) + d_\mu\bar{N}_\mu^1(k'\bar{r})], \quad (12a)$$

where μ incorporates the indices σ, m, n, and c_μ and d_μ are unknown coefficients. $k' = \omega(\mu\epsilon)^{1/2} = (\mu_r\epsilon_r)^{1/2}k$. The $\bar{H}$ field internal to S is given by

$$\bar{H}(k'\bar{r}) = \frac{1}{j\omega\mu}[\nabla\times\bar{E}(k'r)]$$

$$= -j\left(\frac{\epsilon_r}{\mu_r}\right)^{1/2}\left(\frac{\epsilon_0}{\mu_0}\right)^{1/2}\sum_{\mu=1}^{N}[c_\mu\bar{N}_\mu^1(k'\bar{r}) + d_\mu\bar{M}_\mu^1(k'\bar{r})]. \quad (12b)$$

V. Application of the Boundary Conditions at the Surface

The boundary conditions at the surface require that the tangential components of the fields be continuous, i.e.,

$$\bar{n}\times\bar{H}_+ = \bar{n}\times\bar{H}_- \quad (13a)$$

and

$$\bar{n}\times\bar{E}_+ = \bar{n}\times\bar{E}_-. \quad (13b)$$

The plus (+) sign and minus (−) sign subscripts on the surface fields indicate that these fields are the external and internal fields, respectively, evaluated at the surface. From Eq. (12), the tangential components of the internal fields evaluated at the surface are

$$\bar{n}\times\bar{E}_- = \sum_{\mu=1}^{N}[c_\mu\bar{n}\times\bar{M}_\mu^1(k'\bar{r}') + d_\mu\bar{n}\times\bar{N}_\mu^1(k'\bar{r}')], \quad (14a)$$

$$\bar{n}\times\bar{H}_- = -j\left(\frac{\epsilon_r}{\mu_r}\right)^{1/2}\left(\frac{\epsilon_0}{\mu_0}\right)^{1/2}\sum_{\mu=1}^{N}[c_\mu\bar{n}\times\bar{N}_\mu^1(k'\bar{r}') + d_\mu\bar{n}\times\bar{M}_\mu^1(k'\bar{r}')]. \quad (14b)$$

Now, due to the equality of the tangential surface fields in Eqs. (13), Eqs. (14) can now be substituted into the first $2N$ of Eqs. (11), giving the system of equations,

$$\left[K + \left(\frac{\epsilon_r}{\mu_r}\right)^{1/2}J\right]c_\mu + \left[L + \left(\frac{\epsilon_r}{\mu_r}\right)^{1/2}I\right]d_\mu = -ja_\nu \quad \nu = 1, 2, \ldots, N, \quad (15a)$$

$$\left[I + \left(\frac{\epsilon_r}{\mu_r}\right)^{1/2}L\right]c_\mu + \left[J + \left(\frac{\epsilon_r}{\mu_r}\right)^{1/2}K\right]d_\mu = -jb_\nu, \quad (15b)$$

where

$$I = \frac{k^2}{\pi}\int_S \bar{n}\cdot\bar{M}_\nu^3(k\bar{r}')\times\bar{M}_\mu^1(k'\bar{r}')dS,$$

$$J = \frac{k^2}{\pi}\int_S \bar{n}\cdot\bar{M}_\nu^3(k\bar{r}')\times\bar{N}_\mu^1(k'\bar{r}')dS,$$

$$K = \frac{k^2}{\pi}\int_S \bar{n}\cdot\bar{N}_\nu^3(k\bar{r}')\times\bar{M}_\mu^1(k'\bar{r}')dS,$$

$$L = \frac{k^2}{\pi}\int_S \bar{n}\cdot\bar{N}_\nu^3(k\bar{r}')\times\bar{N}_\mu^1(k'\bar{r}')dS.$$

These are a set of simultaneous linear equations that can be solved for the expansion coefficients of the internal field. Subsequent analysis will provide a relationship between these coefficients and the expansion coefficients of the scattered field.

VI. Evaluation of the Scattered Field

The coefficients of the internal field can be obtained by solution of Eqs. (15). These coefficients can then be used in Eqs. (14) to find $\bar{n}\times\bar{E}_-$ and $\bar{n}\times\bar{H}_-$, which when substituted into Eq. (4) will give the expression for the scattered field.

$$\bar{E}^s(k\bar{r}) = \sum_{\nu=1}^{N}[p_\nu\bar{M}_\nu^3(k\bar{r}) + q_\nu\bar{N}_\nu^3(k\bar{r})], \quad (16)$$

where r is outside a circumscribed sphere,

$$p_\nu = -jD_\nu\sum_{\mu=1}^{N}\left\{\left[K' + \left(\frac{\epsilon_r}{\mu_r}\right)^{1/2}J'\right]c_\mu + \left[L' + \left(\frac{\epsilon_r}{\mu_r}\right)^{1/2}I'\right]d_\mu\right\}, \quad (17a)$$

$$q_\nu = -jD_\nu \sum_{\mu=1}^{N} \left\{ \left[I' + \left(\frac{\epsilon_r}{\mu_r}\right)^{1/2} L' \right] c_\mu + \left[J' + \left(\frac{\epsilon_r}{\mu_r}\right)^{1/2} K' \right] d_\mu \right\}, \quad (17b)$$

and

$$I' = \frac{k^2}{\pi} \int_S \bar{n} \cdot \bar{M}_\nu^1(k\bar{r}') \times \bar{M}_\mu^1(k'\bar{r}')dS,$$

$$J' = \frac{k^2}{\pi} \int_S \bar{n} \cdot \bar{M}_\nu^1(k\bar{r}') \times \bar{N}_\mu^1(k'\bar{r}')dS,$$

$$K' = \frac{k^2}{\pi} \int_S \bar{n} \cdot \bar{N}_\nu^1(k\bar{r}') \times \bar{M}_\mu^1(k'\bar{r}')dS,$$

$$L' = \frac{k^2}{\pi} \int_S \bar{n} \cdot \bar{N}_\nu^1(k\bar{r}') \times \bar{N}_\mu^1(k'\bar{r}')dS.$$

The vector far-field amplitude of the scattered field is defined by

$$\bar{E}^s(k\bar{r}) = \bar{F}(\theta_s, \phi_s/\theta_i, \phi_i)\frac{\exp(jkr)}{r}, kr \longrightarrow \infty, \quad (18)$$

where $\bar{F}(\theta_s, \phi_s/\theta_i, \phi_i)$ is the vector far-field amplitude in the (θ_s, ϕ_s) direction due to an incident field in a given (θ_i, ϕ_i) direction.

The differential scattering cross section is defined as

$$\sigma_D = \lim_{r\to\infty} \left[4\pi r^2 \frac{S_s(\theta_s, \phi_s)}{S_i(\theta_i, \phi_i)} \right], \quad (19)$$

where $S_s(\theta_s, \phi_s)$ = the scattered power density

$$= \frac{|\bar{F}(\theta_s, \phi_s/\theta_i, \phi_i)|^2}{2Z_0 r^2}, Z_0 = \sqrt{\mu_0/\epsilon_0},$$

and $S_i(\theta_i, \phi_i)$ = the incident power density

$$= \frac{|\bar{E}^i|^2}{2Z_0}.$$

Assuming that the incident electric field $\bar{E}^i$ has unit amplitude and substituting the expression for S_s and S_i into Eq. (19) give

$$\sigma_D(\theta_s, \phi_s/\theta_i, \phi_i) = 4\pi|\bar{F}(\theta_s, \phi_s/\theta_i, \phi_i)|^2. \quad (20)$$

For $(\theta_s, \phi_s) = (\pi - \theta_i, \pi + \phi_i)$, this reduces to the usual definition for backscatter cross section.

VII. Computed Results

The equations of the previous sections have been solved numerically on a digital computer to investigate the dependence of the differential scattering characteristics of closed three-dimensional bodies on the size, shape, and dielectric constant of the scattering object.

The method of numerical solution for a particular scattering problem consists of choosing a value for N, solving the set of equations for the differential scattering cross section, then repeating the calculation for successively larger N values until the final result (the differential scattering cross section) converges to a specified accuracy. The maximum value of N required for a given problem is dependent on the shape (deviation from a sphere), size, and index of refraction. Small spheres with an index of refraction near unity require small values of N, while a large cylinder with relatively high index of refraction would require a much larger N value for solution. This characteristic of the numerical solution accounts for the suitability of this method to resonance-sized objects. The scattering by smaller objects can be solved more simply by the Rayleigh approximation, and, although large objects can be handled by this method, the large number of terms required will in many cases result in a very large mathematical problem that might be better solved by geometrical optics methods.

The validity of the computational procedure was first verified by making calculations for spherical bodies and comparing the results to those obtained by the Mie theory. After satisfactory results for this test were obtained, the validity check was extended to nonspherical shapes by computing the scattering due to a sphere with the origin of the sphere moved off-center. This has the effect of making the sphere appear nonspherical as far as the mathematics is concerned, however, the computer program must still calculate the same scattered field as is obtained with the origin at the center. Further tests were made including compliance with the law of reciprocity. Specifically, scattering calculations were made for a prolate spheroid wherein the scattered return in one direction due to an incident wave from another direction was compared to the scattered return in the original incident field direction due to an incident wave from the original scattered direction. The scattered field obtained from the two cases was identical.

In this paper we will be concerned with the scattering by axisymmetric bodies, i.e., those bodies having the z axis as an axis of revolution. Specifically, the differential scattering will be evaluated for spheres, prolate and oblate spheroids, and finite cylinders. The scattered field will be evaluated over two planes, which can be called the azimuthal plane and the equatorial plane. The incident wave is defined to be in the (θ_i, ϕ_i) direction and the scattered wave in the (θ_s, ϕ_s) direction. Referring to Fig. 1, the azimuthal and equatorial planes are given as follows:

Azimuthal plane—the incident wave is in the (0°, 0°) direction, i.e., traveling along the z axis in the $+z$ direction. The scattered field is in the $(\theta_s, 0°)$ direction where θ_s varies from 0° to 180°. Therefore, the scattered field is evaluated over that half of the x-z plane lying on the $+x$ side of the origin.

Equatorial plane—the incident wave is in the (90°, 0°) direction, i.e., traveling along the x axis in the $+z$ direction. The scattered field is in the $(90°, \phi_s)$ direction where ϕ_s varies from 0° to 180°. Therefore, the scattered field is evaluated over that half of the x-y plane lying on the $+y$ side of the origin.

The curves of differential scattering cross section vs scattering angle will conform to the convention

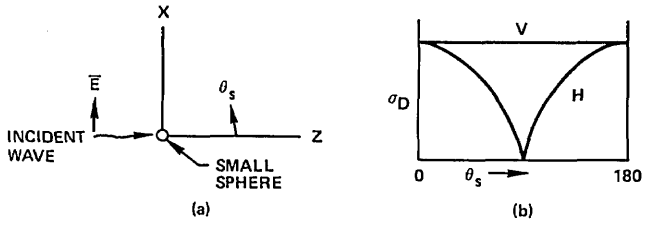

Fig. 7. Rayleigh scattering.

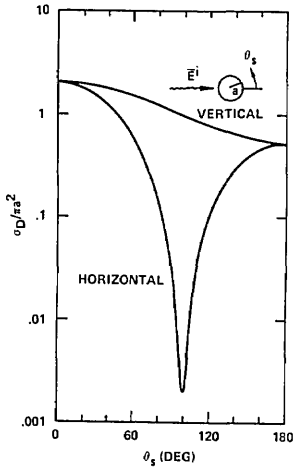

Fig. 8. Sphere scattering, $ka = 1.0$, $\epsilon_r = 4.0$.

used in light scattering studies where the scattering results are plotted from the forward direction to the backward direction, i.e., $\theta_s = 0°$ defines the forward scatter and $\theta_s = 180°$ the backscatter. The scattering angle is plotted along the horizontal axis. The vertical axis is the normalized differential scattering cross section defined as σ_D [see Eq. (20)] divided by πa^2, where a is some characteristic dimension of the scatterer that will be defined in each case. The polarization of the incident and scattered fields will be referred to as either vertical, which is perpendicular to the scattering plane, or horizontal, which is parallel to the scattering plane. It should be noted that for the particular case of the scattering by axisymmetric bodies evaluated over the given planes, symmetry considerations indicate that no cross polarized return will be generated, i.e., a vertically polarized incident wave will generate only a vertically polarized scattered wave and likewise for the horizontally polarized wave case.

Before looking at the results for nonspherical bodies, it will be useful to examine the behavior of the differential scattering curves for lossless dielectric spheres. For spheres lying in the Rayleigh region, the scattered field will be the same as that of a small electric dipole as shown in Fig. 7.

For the horizontally polarized incident wave shown, the differential scattering cross section in the x-z plane is given by curve H in Fig. 7(b). The curve due to a vertically polarized incident wave is a straight line in this plane.

Keeping the dielectric constant the same and increasing the size of the sphere result in a more complex interaction, and the differential scattering curve starts to change in a predictable manner. The curve in Fig. 7 would apply to a sphere with ka (a = the radius) no greater than about 0.157. The curve for $ka = 1.0$, $\epsilon_r = 4.0$, which is given in Fig. 8, shows that for a slightly larger sphere, the scattering starts to peak in the forward direction. This forward peak is a characteristic trait of all larger spheres.

Figure 9 shows the vertical polarization differential scattering curve for spheres of size $ka = 3$ and 5, where the dielectric constant is held to $\epsilon_r = 4.0$. A series of maxima and minima have begun to appear in the backward direction, and, as the size is increased, they move toward the forward direction, and additional maxima and minima arise in the backward direction. Qualitatively, it is observed that the larger the sphere, the more peaks and valleys are evident in the vertical polarization differential scattering curve. A similar effect occurs for the horizontally

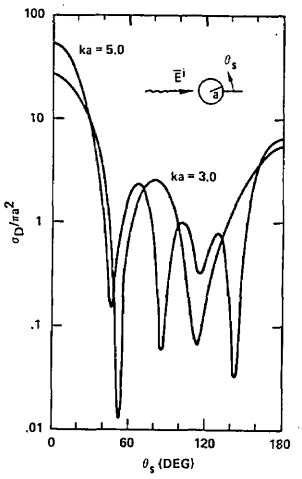

Fig. 9. Sphere scattering, vertical polarization, $ka = 3.0, 5.0$, $\epsilon_r = 4.0$.

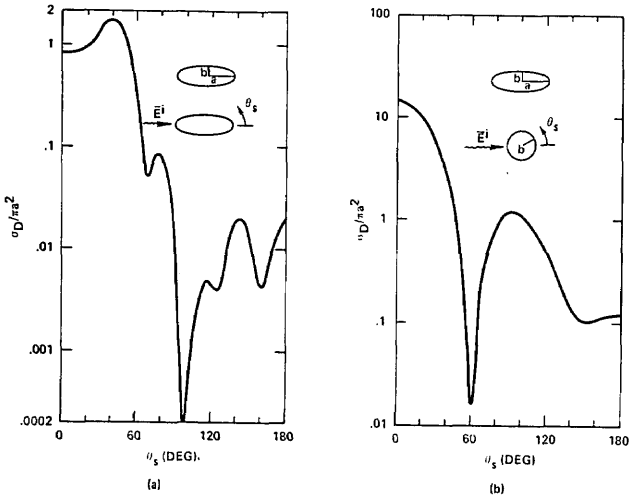

Fig. 10. 3:1 prolate spheroid scattering, vertical polarization, $ka = 7.114$, $\epsilon_r = 5.0$: (a) azimuthal plane; (b) equatorial plane.

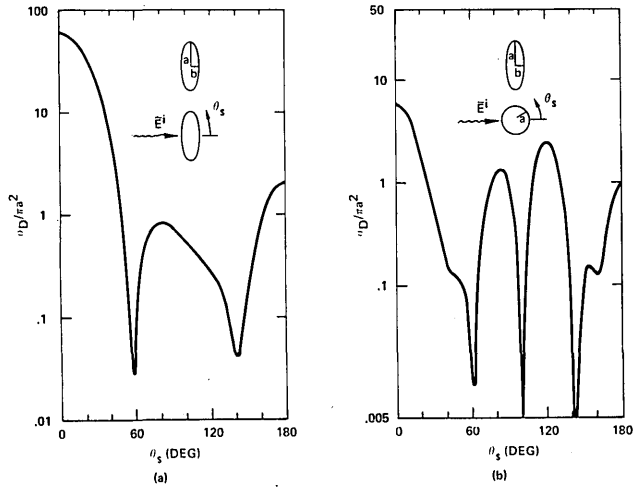

Fig. 11. 3:1 oblate spheroid scattering, vertical polarization, ka = 4.932, ϵ_r = 5.0: (a) azimuthal plane; (b) equatorial plane.

polarized return; however, the amplitude of the oscillation is not as great as in the vertically polarized case, and other effects take place that are not as predictable as in the vertical polarization case. For a different dielectric constant, the behavior of the scattering pattern with increasing size is similar, i.e., more peaks and valleys appear for larger spheres.

The vertical polarization scattering curves for a 3:1 prolate spheroid are given in Figs. 10(a) and 10(b) for the azimuthal and equatorial planes, respectively. One very interesting phenomenon is observed. The azimuthal plane scattering curve [Fig. 10(a)] oscillates rather rapidly with scattering angle and qualitatively is very similar to the return that might be expected from a relatively large sphere. On the other hand, the scattering curve in the equatorial plane [Fig. 10(b)] has fewer oscillations similar to that which one might expect from a relatively smaller sphere. The differential scattering characteristics apparently indicate some measure of size of the scatterer in the direction in which the incident wave is traveling. This behavior was further examined by repeating the calculation for a 3:1 oblate spheroid. These results are shown in Fig. 11. As expected, the curve in the azimuthal plane has fewer oscillations than the curve over the equatorial plane, because the scattering in the azimuthal plane is primarily influenced by the thickness of the spheroid along the minor axis while the equatorial plane scattering is dependent on the major axis thickness. This measurement theory is very interesting, because it indicates a method of experimentally obtaining relative size and shape information for nonspherical particles. (The experimental measurement procedure is a problem unto itself.) Another interesting feature of the scattering behavior is evident in Fig. 10(a). The peak in the curve at 40° is a characteristic that is not expected based on experience with spherical scatterers, where the peak return usually occurs in the forward direction (0°). The peak here is believed due to a specular reflection off the leading edge of the spheroid.

Discussion in the preceding paragraph has concluded that the scattering in a given plane is dependent on the features of the scatterer in that plane. It will be interesting to determine to what extent the scattering in one plane is dependent on the physical features of the scatterer in another plane. Figure 12 shows the differential scattering in the equatorial plane for 2:1 and 3:1 capped cylinders with the same minor diameters, but different lengths. It can be seen that both vertical and horizontal curves are almost identical in shape. Calculations were also made for a shorter cylinder (1.5:1) with the same minor diameter, and the scattering curves, although similar to the 2:1 curves in Fig. 12(a), did not have the almost exact correlation that is evident for the 2:1 and 3:1 cylinders. The conclusion is that the scatter-

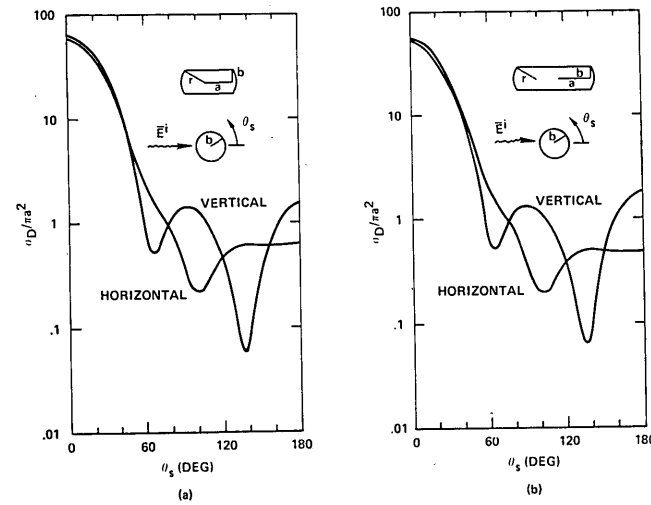

Fig. 12. Cylinder scattering, equatorial plane, ϵ_r = 1.96, r = 2b: (a) 2:1, ka = 5.288, b/a = 0.577; (b) 3:1, ka = 8.341, b/a = 0.366.

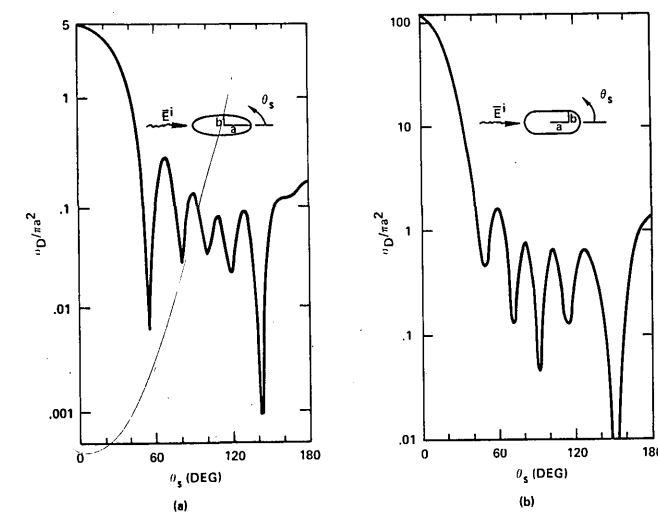

Fig. 13. Scattering by similar bodies, vertical polarization, azimuthal plane, ϵ_r = 2.28: (a) 2:1 prolate spheroid, ka = 9.529, a/b = 2.0; (b) 2:1 cylinder, ka = 4.765, a/b = 1.0.

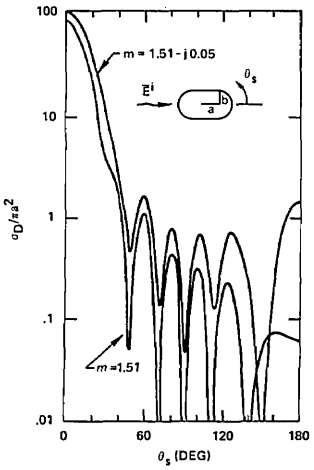

Fig. 14. Cylinder scattering, azimuthal plane, $ka = 4.765$, $a/b = 1.0$, $m = 1.51$, $m = 1.51 - j0.05$.

ing in the equatorial plane becomes independent of length for longer cylinders.

To further investigate the dependence of the differential scattering curves on shape, a calculation was made for a prolate spheroid and a capped cylinder, both bodies having the same length and width (and dielectric constant). The prolate spheroid vertical polarization scattering curve for the azimuthal plane is shown in Fig. 13(a), and that for the cylinder is given in Fig. 13(b). It can be seen that even with the same over-all dimensions, small variations in shape cause quite noticeable differences in the differential scattering characteristics.

Figure 14 compares the vertical polarization differential scattering curves for a lossless cylinder (real index of refraction) and for the same cylinder with a small amount of loss added (complex index of refraction). The behavior of the curves is very similar to that which is observed for spherical scatterers. It can be seen that the absorption has caused a change in the differential scattering characteristic that is manifested primarily by a reduction in the scattered energy all the way around the cylinder, although the effect of the internal loss is much more noticeable in the backscatter direction than in the forward direction. The reason for this is probably attributable in part to a diffraction of a large percentage of the incident radiation around the edge of the cylinder. This component is unaffected by the internal features and therefore shows no reduction when the interior becomes absorbing. The small reduction in the forward direction is due to that portion of the forward scattered wave that is refracted through the cylinder, while a major portion of the backscattered energy is due to that portion of the incident wave that is refracted into the interior region and then exists in the backward direction after multiple internal reflections. This component is directly dependent on the internal characteristics of the scattering object and therefore is attenuated when loss is added. The net effect of all this is that the effect of loss in the interior is much more noticeable in the backward than in the forward directions.

This is illustrated very graphically by looking at the ratio of forward to backscatter in the two cases. That ratio is 80 in the lossless case and almost 1500 in the lossy case.

VIII. Conclusion

The differential scattering of electromagnetic plane waves by homogeneous isotropic dielectric bodies has been theoretically investigated. The numerical results obtained here have investigated the dependence of the scattering on the physical characteristics of the scatterer. The analytical method has wide application to many physical problems including those where the scattering by known objects must be determined (the direct scattering problem) and those where theoretical results are needed for comparison to experimental scattering results to determine the characteristics of unknown scatterers (the inverse scattering problem). An example of the former would be in the area of atmospheric physics where the interaction of various types of electromagnetic waves with aerosols is required. The solution of the inverse problem is required in the study of small chemical and biological particles by light scattering methods.

The authors express their sincere appreciation to P. C. Waterman of the Mitre Corporation and P. J. Wyatt of Science Spectrum, Incorporated, for their interest in this project and their valuable comments.

References

1. M. Kerker, *The Scattering of Light and Other Electromagnetic Radiation* (Academic, New York, 1969).
2. R. G. Kouyoumjian, L. Peters, Jr., and D. T. Thomas, IEEE Trans. Antennas Propag. **AP-11**, 690 (1963).
3. J. B. Keller, J. Opt. Soc. Am. **52**, 116 (1962).
4. R. F. Harrington, *Time-Harmonic Electromagnetic Fields* (McGraw-Hill, New York, 1961).
5. C. Yeh, J. Opt. Soc. Am. **55**, 309 (1965).
6. J. A. Stratton, *Electromagnetic Theory* (McGraw-Hill, New York, 1941).
7. R. H. T. Bates, J. R. James, I. N. L. Gallett, and R. F. Millar, Radio Electron. Eng. **43**, 193 (1973).
8. D. R. Wilton and R. Mittra, *IEEE Trans. Antennas Propag.* **AP-20**, 310 (1972).
9. C. Yeh, Phys. Rev. **135**, A1193 (31 August 1964).
10. J. H. Richmond, IEEE Trans. Antennas Propag. **AP-13**, 334 (1965).
11. J. H. Richmond, Proc. IEEE **53**, 796 (1965).
12. P. C. Waterman, Proc. IEEE **53**, 805 (1965).
13. P. C. Waterman and C. V. McCarthy, "Numerical Solution of Electromagnetic Scattering Problems," Mitre Corporation, Bedford, Massachusetts, Report MTP-74 (N69-31912) (June 1968).
14. P. C. Waterman, Alta Freq. **38** (Speciale), 348 (1969).
15. P. C. Waterman, Phys. Rev. D **3**, 825 (1971).
16. H. Honl, A. W. Maue, and K. Westpfahl, *Handbuch der Physik* (Springer Verlag, Berlin, 1961), Vol. 25/1.
17. S. A. Schelkunoff, *Electromagnetic Waves* (D. Von Nostrand, New York, 1943).
18. P. M. Morse and H. Feshbach, *Methods of Theoretical Physics* (McGraw-Hill, New York, 1953).
19. A. Nehari, *Introduction to Complex Analysis* (Allyn and Bacon, Boston, Mass., 1968).